Carcinogenesis vol.17 no.4 pp.815–820, 1996

Involvement of glutathione in induction of c-*jun* proto-oncogene by methylmethanesulfonate in NIH 3T3 cells

Min-Liang Kuo, Tzu-Ching Meng[1] and Jen-Kun Lin[2]

Institute of Toxicology, [2]Institute of Biochemistry, College of Medicine, National Taiwan University, no. 1, Section 1, Jen-Ai Road, Taipei, Taiwan and [1]Department of Biochemistry and Molecular Biology, University of Nebraska Medical Center, Omaha, NE 68198, USA

The c-*jun* proto-oncogene plays a vital role in the carcinogenic process. Although numerous works have extensively investigated the induction mechanisms of c-*jun* by UV, hydrogen peroxide or 12-*O*-tetradecanoylphorbol-13-acetate, the mechanism induced by alkylating agents has received little attention. In this study, NIH 3T3 cells were exposed to methylmethanesulfonate (MMS), revealing that the agent clearly induced c-*jun* expression with a peak at 2 h. Pretreatment of cells with various kinase inhibitors, e.g. H7, genistein, herbimycin A and tyrphostin, did not show any significant effects on the MMS-induced c-*jun* expression. Benzamide, an inhibitor of poly(ADP)-ribosylation, enhanced the MMS-induced DNA breakages, but did not potentiate that agent which elicited c-*jun* expression. Another experiment showed that this agent transfected and overexpressed an activated v-H-*ras* gene in NIH 3T3 cells, which became more resistant to MMS-induced DNA damage but expressed the same level of c-*jun* transcript as compared with NIH 3T3 cells in response to MMS. If intracellular glutathione (GSH) was completely depleted by buthionine sulfoximine (BSO), the MMS-elicted c-*jun* expression was blocked. Subsequently, re-elevating intracellular GSH by washing off BSO caused the expression of c-*jun* by MMS to increase proportionately. Based on these findings, we can conclude that the mechanism by which MMS induced c-*jun* expression does not occur through activation of protein tyrosine kinases or initiation of DNA damage, but is closely related to the intracellular GSH.

Introduction

The c-*jun* proto-oncogene, which encodes a component of transcriptional activator complex AP-1 (1), has been shown to be rapidly induced in mammalian cells in response to various stimuli, including UV (2), phorbol esters (3), oxidative stresses (4) and DNA-damaging compounds (5). Continuous expression of c-*jun* results in transformation of fibroblasts in culture and the induction of tumors in animals (6,7). Introducing a mutant of c-*jun* could block *ras* plus SV40 large T antigen or tumor promoter 12-*O*-tetradecanoylphorbol-13-acetate (TPA*)-induced rat embryo cell transformation (8). Recently, Dong *et al.* (9) showed that retinoic acid is active in inhibiting TPA-induced anchorage-independent transformation of JB6 P^+ cells in the dose range that blocks TPA-induced AP-1 activity. This would suggest that a specific block in induced AP-1 activity inhibits tumor promoter-induced transformation. In agreement with this finding, curcumin, a potent inhibitor of tumor promotion, suppresses TPA-induced c-*jun* expression in mouse fibroblasts (10). Furthermore, a persistent induction of c-*jun* and c-*fos* was observed in asbestos-treated mesothelial cells, thereby suggesting that asbestos-induced carcinogenesis would be involved in chronic stimulation of cell proliferation through activation of c-*jun* and/or c-*fos* proto-oncogenes (11). Taken together, the evidence strongly suggests that the c-*jun* proto-oncogene plays a crucial role in the process of carcinogenesis. In addition to carcinogenesis, c-*jun* has recently been reported to be involved in apoptotic cell death (12) and cell differentiation (13).

Recent investigations have focused primarily on which signal pathways may participate in regulating c-*jun* expression in response to various stimuli. For example, Curran *et al.* (14) successfully demonstrated that the DNA-binding activity of AP-1 is regulated by a novel redox mechanism. Furthermore, a key regulatory 37 kDa protein (Raf-1) corresponding to the redox factor was subsequently identified, suggesting that Raf-1 may represent a novel redox component of the signal transduction processes that regulate c-*jun* expression. Another study showed that activation of Src tyrosine kinases was the earliest step for induction of c-*jun* by UV, followed by activation of Ha-Ras and Raf-1 (15). However, some contradictory findings (16) suggest that UV initially elicited a signal from DNA damage occurring at a nuclear site, subsequently transducing the signal to cytoplasm and ultimately activating Raf-1 and MAP-2 kinases. Membrane-activated protein kinase, such as protein kinase C, has also been reported to serve as a primary target in the signal pathway leading to c-*jun* induction in response to TPA treatment (17). Consequently, this signal converges upon Raf-associated pathways.

Although many studies have elucidated the possible mechanisms involved in c-*jun* induction in response to UV or TPA, little is known about the signal transduction mechanisms of c-*jun* induced by alkylating compounds. Therefore, in this study we examine which cellular components may be involved in induction of c-*jun* by methylmethanesulfonate (MMS). The results obtained here indicate that the level of small peptide glutathione (GSH) within cells may play an important role in regulating this induction.

Materials and methods

Cell cultures and chemicals

NIH 3T3 cells and v-H-*ras* oncogene-transformed NIH 3T3 cells (a gift from Dr S.-F.Yang of the Institute of Molecular Biology, Academia Sinica, Taiwan) were grown in Dulbecco's modified Eagle's medium containing 10% fetal calf serum, 100 U/ml penicillin and 100 U/ml streptomycin. TPA, H7, tyrphostin, herbimycin A, genistein and buthionine sulfoximine (BSO) were purchased from Sigma Chemical Co. (St Louis, MO). MMS was obtained from Aldrich Co. (Milwaukee, WI).

Determination of single strand breaks (SSBs) in DNA

The number of SSBs was determined using the alkaline unwinding technique described by Solveing Walles and Erixon (18). Briefly, cells (1×10^6) were

Abbreviations: TPA, 12-*O*-tetradecanoylphorbol-13-acetate; MMS, methylmethanesulfonate; GSH, glutathione; BSO, L-buthionine-*SR*-sulfoximine; PKC, protein kinase C; IL-2, interleukin 2; HMPS, hexose monophosphate shunt.

washed with PBS and digested with 1 × trypsin–EDTA, then treated with 30 mM NaOH, 0.15 M NaCl at room temperature for 10 min in the dark. The alkaline unwinding was terminated by adding the neutralizing solution (0.02 M NaH_2PO_4) to pH 6.8. The solution was treated with a brief ultrasonication (40 W, 15 s) before adding SDS to a final concentration of 0.25 g/100 ml The sample could be stored deep-frozen or be put on glass columns of hydroxylapatite (10 × 150 mm; Bio-Gel HTP; DNA-grade Bio-Gel = 2:1; Bio-Rad; 0.3 g per column) at 60°C. The column was washed with 10 ml 0.02 M NaH_2PO_4 (pH 6.8). Next, the single and double strand DNA were eluted with 5 ml 0.08 M and 0.25 M KH_2PO_4 (pH 6.8) respectively. DAPI was added and the amount of DNA was measured by fluorimetry under an excitation wavelength of 373 nm; the absorbance of emission (Ab) was detected at 454 nm. The number of SSBs was reflected in the percentage of single-strand DNA calculated from the following equation: [Ab_{454nm} of single-strand DNA]/[Ab_{454nm} of (single-strand DNA + double-strand DNA)] × 100%.

Determination of the intracellular GSH content

Total intracellular GSH content was measured using the enzyme recycling assay (19). Cells were harvested by trypsinization and cell pellets were resuspended in 0.5 ml 2% sulfosalicylic acid (Sigma) and subjected three times to rapid freeze–thaw lysis. Particulate matter was separated by centrifugation at 4000 *g*, and protein-free lysate was then obtained from the supernatant and used for GSH measurement while the pellet was dissolvd in 1 M NaOH and analyzed for protein by the Bio-Rad assay kit. GSH content was calculated from the rate of change in absorbance at 412 nM on the basis of the standard curve in each experiment.

Hybridization probe

A full-length *Eco*RI fragment of c-*jun* coding sequence (20) and a GAPDH cDNA *Pst*I fragment cut out from pIBI30 GAPDH (21) were used as hybridization probes. DNA fragments were purified by electrophoresis on NA-45 membranes (Schleicher and Schuell) and radiolabeled by a random primer kit (New England Biotechnology) using [α-^{32}P]dCTP (Amersham).

Total RNA isolation and Northern blot analysis

Total cellular RNA was isolated as described by Xie and Rothblum (22). For Northern blots, RNA (20 µg/lane) was separated in an agarose/formaldehyde gel, transferred to Zeta-probe nylon filter (Bio-Rad), and hybridized to the DNA probes (1–2 × 10^6 c.p.m./ml). The filter was washed successively in 2 × SSC, 0.1% SDS; 0.5 × SSC, 0.1% SDS and 0.1 × SSC, 0.1% SDS for 15 min in each solution at 65°C, followed by exposure on X-ray film (Kodak XAR-5) with an intensifying screen at −70°C. Finally, the X-ray film was developed and scanned to estimate the band density.

Results

A kinetics study of c-jun induction by MMS, H_2O_2 and TPA

The time course of c-*jun* induction by 1 mM MMS is shown in Figure 1A. A peak of c-*jun* induction was observed at 2 h after compound treatment. Consequently, the level of c-*jun* decreased gradually and returned to a control level by 8 h. For reference, the response of c-*jun* to MMS was compared with its induction by hydrogen peroxide (H_2O_2) and TPA. As shown in Figure 1(B,C), in response to H_2O_2 and TPA c-*jun* expression was more rapidly induced with peaks at 30 and 60 min respectively.

Effects of protein kinase inhibitors on MMS-elicited c-jun mRNA expression

Protein kinase C (PKC) (17) and tyrosine kinases (15) have been found to play a prominent role in TPA- and UV-induced c-*jun* activation respectively. In this study, whether or not PKC is involved in c-*jun* induction by MMS is verified by employing long-term exposure (24 h) to TPA or following 1 h pretreatment with H7 (25 µM) to block the PKC activity. These results indicate that neither TPA nor H7 treatment affected c-*jun* induction by MMS (Figure 2, lanes 3 and 4).

Furthermore, three different tyrosine kinase inhibitors, i.e. tyrphostin-23 (50 µM), genistein (50 µM) and herbimycin A (1.5 µg/ml), were used to examine the effects on this induction by MMS. The examination revealed that the induction of

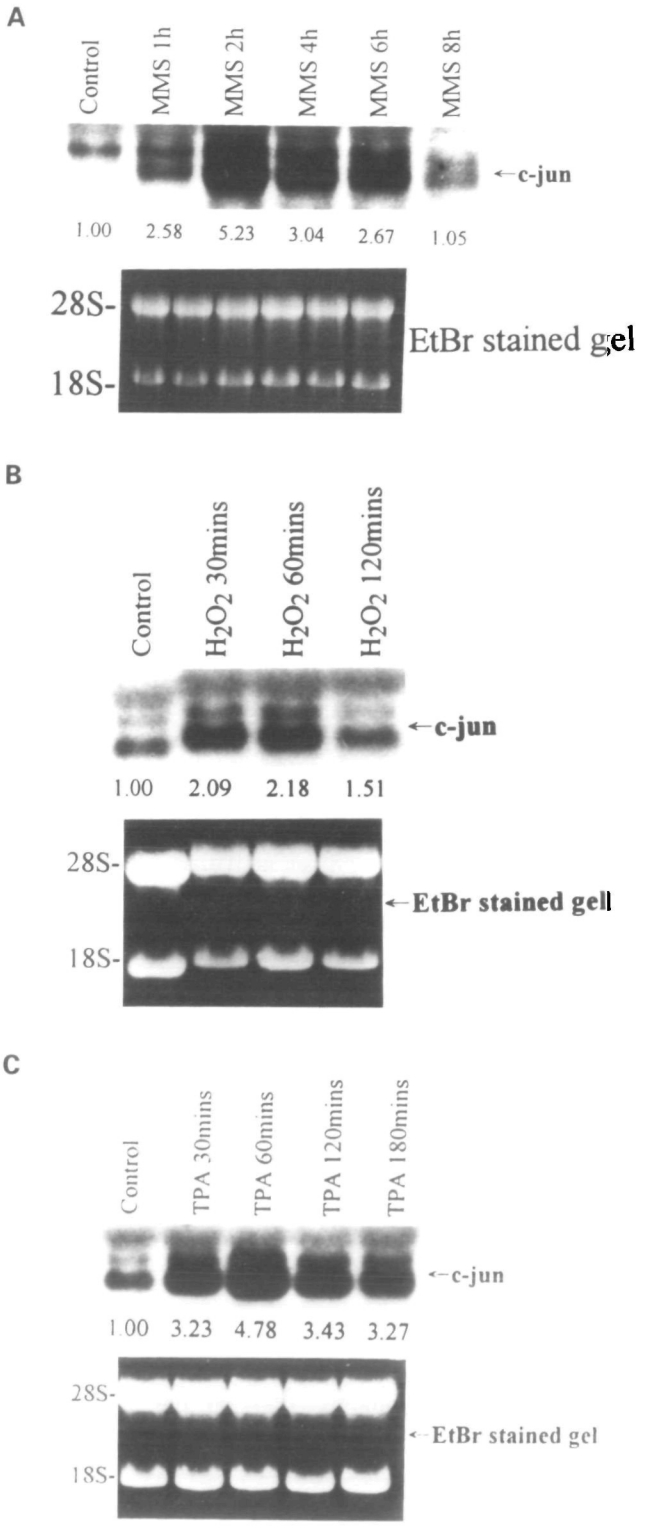

Fig. 1. (A) Kinetics of c-*jun* induction by 1 mM MMS in NIH 3T3 cells. (B) Kinetics of c-*jun* induction by 200 µM H_2O_2 and (C) kinetics of c-*jun* induction by 100 ng/ml TPA in NIH 3T3 cells. Total RNA was extracted from confluent cells cultured in DMEM with 10% serum at different time points of MMS treatment indicated in the figure. Expression of mRNA was analyzed by Northern blots using ^{32}P-labeled cDNA of c-*jun* as hybridizing probe. Next, the membrane was exposed to X-ray film for 72 h. Quantitation of c-*jun* mRNA by densitometric scanning is shown at the bottom of the figure. The number indicates the fold-change of c-*jun* of treated cells versus control cells in the ethidium bromide-stained gel-normalized density of the autoradiogram. Positions of 28S and 18S rRNA are marked on the left

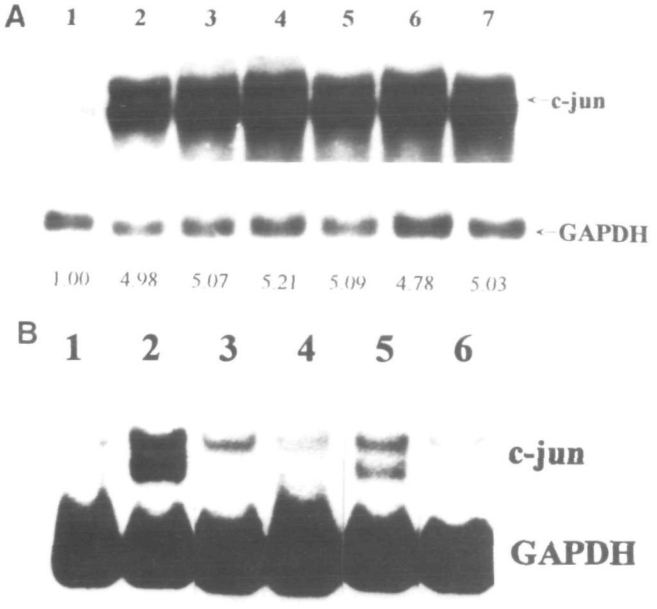

Fig. 2. (**A**) Effects of kinase inhibitors on the MMS-induced expression of c-*jun* in NIH 3T3 cells. Cells were treated as follows: control (**lane 1**); 1 mM MMS for 2 h (**lane 2**); pre-exposure with 100 ng/ml TPA for 24 h (**lane 3**); 25 μM H7 for 1 h (**lane 4**); 50 μM tyrphostin for 1 h (**lane 5**); 1.5 μg herbimycin A for 1 h (**lane 6**) and 50 μM genistein for 1 h (**lane 7**), then 1 mM MMS for another 2 h respectively. (**B**) Kinase inhibitors inhibit TPA and PDGF-induced c-*jun* mRNA accumulation. Cells were treated as follows: control (**lane 1**); 100 ng/ml TPA for 60 min (**lane 2**); pre-exposure with 100 ng/ml TPA for 24 h (**lane 3**); 25 μM H-7 for 1 h (**lane 4**), then 100 ng/ml added for another 1 h respectively; 50 ng/ml PDGF for 1 h (**lane 5**); pretreatment with 1.5 μg/ml herbimycin A for 1 h (**lane 6**), then PDGF added for a further 1 h. Northern blot analysis as described in Materials and methods. Quantitation of c-*jun* mRNA by densitometric scanning is shown at the bottom of the figure. The number indicates the fold-change of c-*jun* transcripts of treated cells from control cells in the GAPDH-normalized density of the autoradiogram.

c-*jun* did not interfere with these kinase inhibitors (Figure 2, lanes 5–7). To verify that the kinase blockers used here were effective, we performed some appropriate controls as follows: (i) 24 h exposure to TPA and 1 h pretreatment with 25 μM H-7 blocked TPA-induced c-*jun* expression (Figure 2B, lanes 2–4); (ii) 1 h pretreatment with 1.5 μg/ml herbimycin A inhibited platelet-derived growth factor-induced c-*jun* mRNA accumulation (Figure 2B, lanes 5 and 6).

Effects of DNA damage on MMS-elicited c-jun mRNA expression

An alkaline unwinding method is used to monitor the extent of DNA damage following MMS mtreatment. Figure 3A shows that DNA breakages increased proportionately with the time of MMS exposure during the first 2 h. In addition, benzamide (4 mM), a poly(ADP)ribosylation transferase inhibitor, was added 5 min prior to MMS, thereby resulting in a significant increase in DNA damage. Under the same treatment protocol, the levels of c-*jun* transcripts were monitored to observe whether these would change. These results indicate that although benzamide could enhance MMS-induced DNA damage, MMS-elicited c-*jun* expression would not be altered (Figure 3B, lanes 5 and 6). However, benzamide alone did not change the abundance of c-*jun* mRNA (Figure 3B, lanes 3 and 4). As previously described (I.W.Chou *et al.*, unpublished observations), v-H-*ras*-transformed NIH 3T3 cells exhibited a striking resistance to MMS-induced cell death as compared

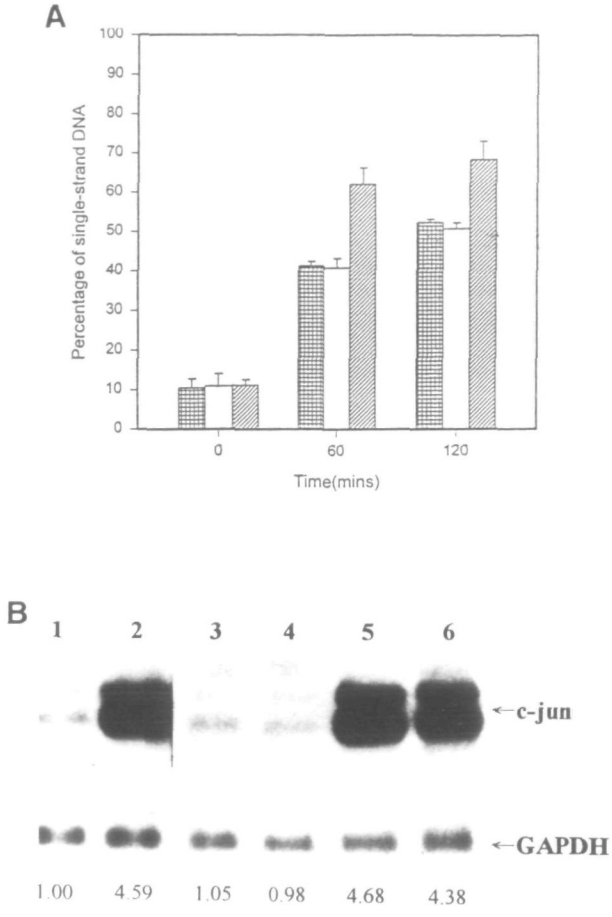

Fig. 3. (**A**) Effects of benzamide on the level of MMS-induced DNA damage measured by alkaline elution at 1 and 2 h of treatment in NIH 3T3 cells. (▦: 1 mM MMS loaded at '0' time; (□: 1 mM benzamide added 5 min before '0' time when 1 mM MMS was loaded; (■) 4 mM benzamide added 5 min before '0' time when 1 mM MMS was loaded. Each point represents the mean of three replicate cultures. (**B**) Effect of benzamide on MMS-induced c-*jun* mRNA expression in NIH 3T3 cells. Total RNA was extracted from cells of the following treatments: **lane 1**, control; **lane 2**, 1 mM MMS for 2 h; **lane 3**, 1 mM benzamide for 2 h; **lane 4**, 4 mM benzamide for 2 h; **lane 5**, 1 mM benzamide for 5 min, then 1 mM MMS added for another 2 h; **lane 6**, 4 mM benzamide for 5 min, then 1 mM MMS added for another 2 h. Methods of Northern blot analysis and quantitation of mRNA were described in Figure 2. Exposure time of X-rays was 96 h.

with their parental NIH 3T3 cells. Consistent with this finding, our results confirmed the absence of DNA breakages in v-H-*ras*-transformed cells during the first 2 h of MMS treatment (Figure 4A). However, the c-*jun* transcript still reached maximal induction at 2 h after MMS treatment (Figure 4B). In addition, it was of interest to note that the induction kinetics of c-*jun* by MMS between NIH 3T3 and v-H-*ras* NIH 3T3 cells was quite similar (Figure 4C). These findings strongly suggest that the induction of c-*jun* by MMS may not occur through DNA damage.

Effects of GSH content on MMS-induced c-jun expression

Intracellular GSH is a preferential target for alkylating agents (23). From this, we postulate that the change of GSH within cells by MMS may be related to its induction of c-*jun*. BSO, a specific inhibitor of γ-glutamylcysteine synthetase, was used to deplete the GSH content within cells to observe its effect on MMS-elicited c-*jun* expression. Exposure of NIH 3T3 cells to 50 or 100 μM BSO for 16 h resulted in a nearly 100%

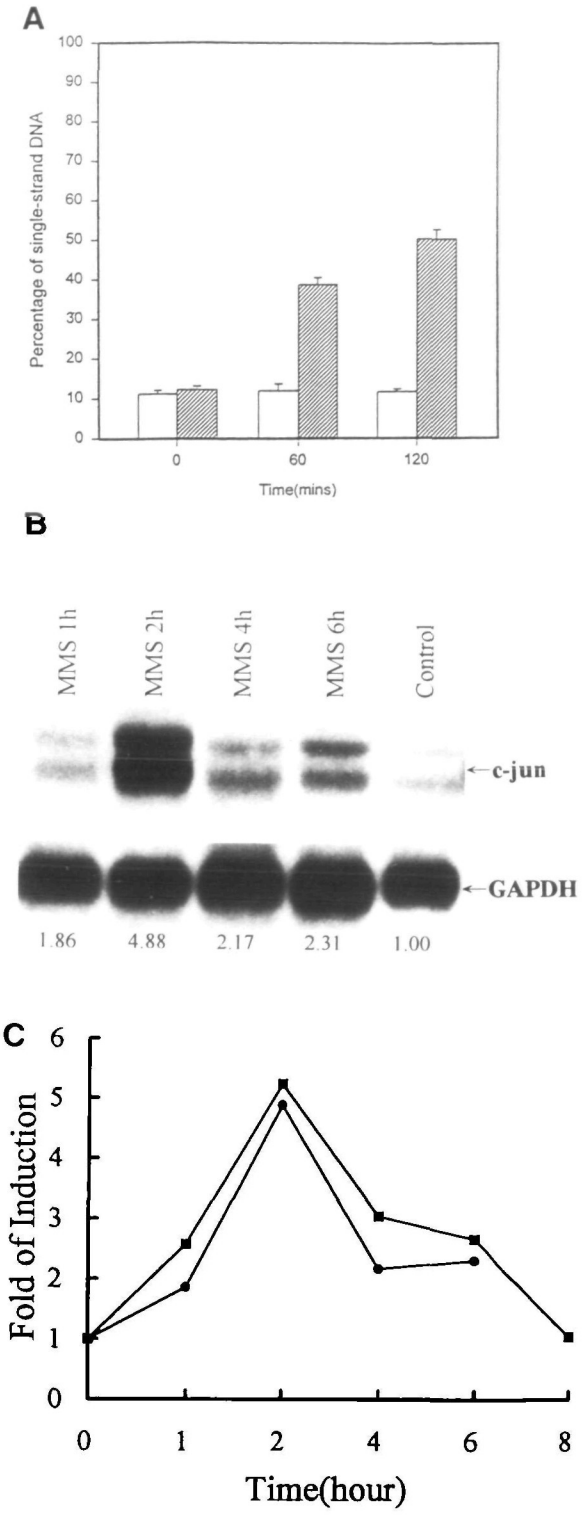

Fig. 4. (A) Difference of 1 mM MMS-induced DNA damage level between parental NIH 3T3 (■) and v-H-*ras*-transformed NIH 3T3 cells (□) during 2 h treatment. Alkaline elution analysis was examined at 0, 60 and 120 min. Each point represents the mean of three replicate cultures. (B) Kinetics of c-*jun* induction by 1 mM MMS in v-H-*ras*-transformed NIH 3T3 cells. Total RNA was extracted at the different time points indicated in the figure and analyzed by Northern blotting. Quantitation of mRNA was measured by the method described in Figure 2. Exposure time of X-rays was 96 h. (C) Comparison of the induction kinetics of c-*jun* mRNA by MMS between NIH 3T3 (■) and v-H-*ras* NIH 3T3 cells (●). The relative induction of c-*jun* between these two cell lines was determined relative to the level of GAPDH signal.

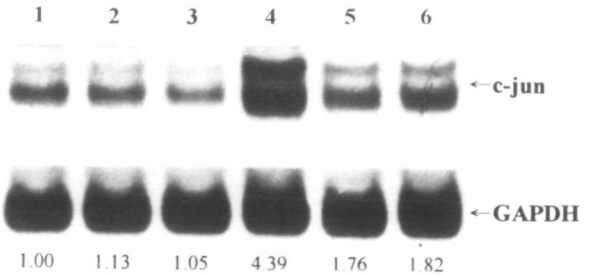

Fig. 5. MMS-induced c-*jun* mRNA expression is inhibited by pretreatment of BSO in NIH 3T3 cells. Total RNA was extracted from the following cells: **lane 1**, control; **lane 2**, 50 μM BSO for 16 h; **lane 3**, 100 μM BSO for 16 h; **lane 4**, 1 mM MMS for 2 h; **lane 5**, 50 μM BSO for 16 h, then 1 mM MMS added for another 2 h; **lane 6**, 100 μM BSO for 16 h, then 1 mM MMS added for another 2 h. Results were measured by Northern blotting. Quantitation of mRNA was measured by the same method described in Figure 2. Exposure time of X-ray film was 48 h.

depletion of GSH (data not shown). Northern blot analysis reveals that treatment of cells with 50 or 100 μM BSO alone did not induce the level of c-*jun* (Figure 5, lanes 2 and 3). However, MMS-induced c-*jun* expression was dramatically inhibited by treatment with BSO (Figure 5, lanes 4–6).

The precise relationship between GSH content and c-*jun* induction by MMS was next determined by depleting intracellular GSH and then re-elevating it by washing off BSO. As shown in Figure 6A, the levels of GSH within cells gradually increased when BSO was washed out. After 24 h of BSO removal, ~80% of GSH was recovered. Next, MMS was added to the cells for 2 h under the same conditions with different levels of GSH as indicated in Figure 6A. These results clearly demonstrated that the expression of c-*jun* by MMS increased proportionately with the elevation of GSH levels (Figure 6B).

Discussion

DNA damage is generally considered to be a primary indication of induction of some specific gene expression by genotoxic compounds (24). However, two lines of evidence presented here demonstrate that c-*jun* induction by MMS may not occur through DNA damage. First, exposure of cells to 4 mM benzamide significantly potentiated the MMS-caused DNA breakages but did not elevate the expression of c-*jun* transcripts. Second, MMS induced less DNA damage in v-H-*ras* NIH 3T3 cells, but elicited a similar level of c-*jun* mRNA as compared to NIH 3T3 cells. TPA- and UV-elicited c-*jun* expression was found to be related to some specific protein kinases. Autophosphorylation of Ltk, which is localized primarily in the endoplasmic reticulum, was dramatically stimulated in response to alkylating and thiol-oxidizing agents (25). In addition, treatment of T cells with either alkylating agents (26) or treatment of early B cells with ionizing radiation (27) increases tyrosine phosphorylation of several cellular proteins. This increase is probably achieved through oxidation or alkylation of a highly reactive essential cysteine residue at tyrosine phosphatase (28). These observations indicate that activation of some protein kinases by changing the phosphorylation status of cellular proteins may function as crucial intermediates in the pathway, thereby leading to c-*jun* induction in response to exogenous stimuli. However, this study failed on multiple trials to affect c-*jun* expression by MMS with some well-known PKC and tyrosine kinase inhibitors. Therefore we

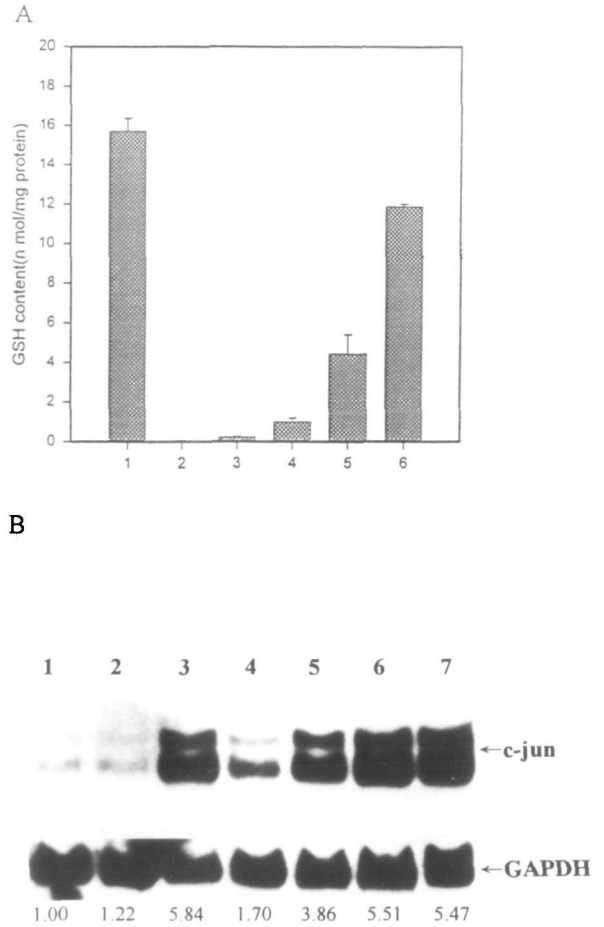

Fig. 6. (**A**) Intracellular GSH content within BSO-treated NIH 3T3 cells recovers gradually after BSO was washed out by fresh medium. GSH content was determined from the following cells: control (**column 1**); 50 μM BSO for 16 h treatment (**column 2**); 50 μM BSO for 16 h treatment, then cells were washed and recultured in fresh medium for another 4 h (**column 3**), 8 h (**column 4**), 16 h (**column 5**) and 24 h (**column 6**) respectively. Each bar represents the mean of three replicate values. (**B**) Expression of MMS-induced c-*jun* mRNA is inhibited by increasing BSO while fresh medium is replaced in NIH 3T3 cells. Total RNA was extracted from the following cells: control (**lane 1**); 50 μM BSO for 16 h treatment (**lane 2**); 1 mM MMS for 2 h treatment (**lane 3**); 50 μM BSO for 16 h treatment then 1 mM MMS for another 2 h (**lane 4**); fresh medium replaced after 16 h treatment of 50 μM BSO for 8, 16 and 24 h, then 1 mM MMS was added for another 2 h (**lanes 5–7** respectively). Northern blots and quantitation of mRNA were performed as described in Figure 2. Exposure time of X-ray film was 72 h.

can conclude that neither PKC nor protein tyrosine kinase is involved in MMS-induced c-*jun* expression.

A large body of evidence suggests that intracellular GSH content plays a vital role in regulating the expression of some genes and a variety of cellular functions. A change in GSH content could affect the actions of interleukin 2 (IL-2) on cytotoxic T cells, including cellular proliferation, efficiency of binding and internalization of IL-2 (29). It has also been reported that depletion of GSH by BSO potentiated the active oxygen species-induced AP-1 binding activity in HepG2 cells (30). Even treatment with BSO alone can also enhance AP-1 binding activity. In contrast, the data in this study demonstrated that the reduction of GSH level by BSO resulted in a decrease in MMS-elicited c-*jun* expression. As the intracellular GSH level was gradually re-elevated by washing off BSO, the MMS-elicited c-*jun* expression increased proportionately (Figure 6B). The concentrations of BSO (50 and 100 μM) used here effectively depleted >90% of intracellular GSH but did not increase in c-*jun* mRNA, thereby suggesting that the change in GSH itself could not alter the c-*jun* expression in this cell line. Based on these findings, we suggest that adducts of GSH and MMS probably play an important role in mediating such a signal transduction pathway.

In agreement with these findings, Clancy *et al.* (32) discovered the depletion of intracellular glutathione was accompanied by a rapid and concomitant activation of the hexose monophosphate shunt (HMPS) following exposure to nitric oxide. Synthetic preparations of *S*-nitrosoglutathione shared with nitric oxide the capacity to activate the HMPS. Therefore, Clancy *et al.* suggested that nitric oxide may regulate cellular functions via the formation of intracellular *S*-nitrosothiol adducts and activation of the HMPS. *S*-Methylglutathione has long been known to inhibit the glyoxalase system (32), indicating that this adduct may exhibit a biological activity in intact cells. Obviously, further research is required to clarify the possible role of methylglutathione in MMS-elicited c-*jun* induction.

To our knowledge, this is the first study to investigate the possible mechanisms involved in c-*jun* induction by chemical carcinogens. Of particular interest is that this induction pathway is not achieved through protein kinase or DNA damage, but is closely related to intracellular GSH levels.

Acknowledgements

This study was supported by the National Science Council, NSC84-2331-B002-035.

References

1. Angel,P., Allegretto,E.A., Okino,S.T., Hattori,K., Boyle,W.J., Hunter,T. and Karin,M. (1988) Oncogene *jun* encodes a sequence-specific trans-activator similar to AP-1. *Nature*, **332**, 166–171.
2. Devary,Y., Gottlieb,R.A., Lau,L.F. and Karin,M. (1991) Rapid and preferential activation of the c-*jun* gene during mammalian UV response. *Mol. Cell. Biol.*, **11**, 2804–2811.
3. Wu,W.S., Lin,J.K. and Wu,F.Y.H. (1992) Differential induction of c-*fos* and c-*jun* proto-oncogenes and AP-1 activity by tumor promoter 12-*O*-tetradecanoylphorbol-13-acetate in cells at different stages of tumor promotion *in vitro*. *Oncogene*, **7**, 2287–2294.
4. Nose,K., Shibanuma,M., Kikuchi,K., Kageyama,H., Sakiyama,S. and Kuroki,T. (1991) Transcriptional activation of early-response genes by hydrogen peroxide in a mouse osteoblastic cell line. *Eur. J. Biochem.*, **201**, 99–106.
5. Manome,Y., Datta,R. and Fine,H.A. (1993) Early response gene induction following DNA damage in astrocytoma cell lines. *Biochem. Pharmacol.*, **45**, 1677–1684.
6. Ransone,L.J. and Verma,I.M. (1990) Nuclear proto-oncogene *fos* and *jun*. *Annu. Rev. Cell Biol.*, **6**, 539–557.
7. Castellazzi,M., Dangy,J.P., Mechta,F., Hirai,S.I., Yaniv,M., Samarut,J., Lassailly,A. and Brun,G. (1990) Overexpression of avian or mouse c-*jun* in primary chick embryo fibroblasts confers a partially transformed phenotype. *Oncogene*, **5**, 1541–1547.
8. Brown,P.H., Alami,R., Preis,L.H., Szabo,E. and Birrer,M.J. (1993) Suppression of oncogene-induced transformation by a deletion mutant of c-*jun*. *Oncogene*, **8**, 877–886.
9. Dong,Z., Birrer,M.J., Watts,R.G., Matrisian,L.M. and Colburn,N.H. (1994) Blocking of tumor promoter-induced AP-1 activity inhibits induced transformation in JBG mouse epidermal cells. *Proc. Natl Acad. Sci. USA*, **91**, 609–613.
10. Huang,T.S., Lee,S.C. and Lin,J.K. (1991) Suppression of c-Jun/AP-1 activation by an inhibitor of tumor promotion in mouse fibroblast cells. *Proc. Natl Acad. Sci. USA*, **88**, 5292–5296.
11. Heintz,N.H., Janssen,Y.H. and Mossman,B.T. (1993) Persistent induction of c-*fos* and c-*jun* expression by asbestos. *Proc. Natl Acad. Sci. USA*, **90**, 3299–3303.

12. Colotta,F., Polentarutti,N., Sironi,M. and Mantorani,A. (1992) Expression and involvement of c-*fos* and c-*jun* protooncogenes in programmed cell death induced by growth factor deprivation in lymphoid cell lines. *J. Biol. Chem.*, **267**, 18278–18283.
13. Angel,P. and Karin,M. (1991) The role of c-*jun*, *fos* and the AP-1 complex in cell-proliferation and transformation. *Biochim. Biophys Acta*, **1072**, 129–157.
14. Xanthoudakis,S. and Curran,T. (1992) Identification and characterization of Raf-1, a nuclear protein that facilitates AP-1 DNA binding activity. *EMBO J.*, **11**, 653–665.
15. Devary,Y., Gottlieb,R.A., Smeal,T. and Karin,M. (1992) The mammalian ultraviolet response is triggered by activation of Src tyrosine kinases. *Cell*, **71**, 1081–1091.
16. Radler-Pohl,A., Sachsenmaier,C., Gebel,S., Auer,H.P., Bruder,J.T., Rapp,U., Angel,P., Rahmsdorf,H.J. and Herrlich,P. (1993) UV-induced activation of AP-1 involves obligatory extranuclear steps including Raf-1 kinase. *EMBO J.*, **12**, 1005–1012.
17. Rahmsdorf,H. and Herrlich,P. (1990) Regulation of gene expression by tumor promoters. *Pharmacol. Ther.*, **48**, 157–188.
18. Solveig Walles,S.A. and Erixon,K. (1984) Single-strand breaks in DNA of various organs of mice induced by methyl methanesulfonate and dimethylsulfoxide determined by the alkaline unwinding technique. *Carcinogenesis*, **5**, 319–323.
19. Griffith,O.W (1980) Determination of glutathione and glutathione disulfide using glutathione reductase and 2-vinylpyridine. *Anal. Biochem.*, **106**, 207–212.
20. Bohmann,D., Bos,T.T., Admon,A., Nishimura,T., Vogt,P.K. and Tjian,R. (1987) Human protooncogene c-*jun* encodes a DNA binding protein with structural and functional properties of transcription factor AP-1. *Science*, **238**, 1386–1392.
21. Piechaczyk,M., Blanchard,J.M., Marty,L., Dany,C., Panabiere,F., Sabouty,S.E., Fort,P. and Jeanteur,P. (1984) Post transcriptional regulation of glyceraldehyde-3-phosphate dehydrogenase gene expression in rat tissue. *Nucleic Acids Res.*, **12**, 6951–6953.
22. Xie,W.Q. and Rothblum,L. (1991) Rapid, small-scale RNA isolation from tissue culture cells. *Biotechniques*, **11**, 324–327.
23. Reitman,F.A., Shertzer,H.G. and Berger,M.L. (1988) Toxicity of methylating agents in isolated hepatocytes. *Biochem. Pharmacol.*, **37**, 3183–3188.
24. Holbrook,N.J and Forance,A.J., Jr (1991) Response to adversity: molecular control of gene activation following genotoxic stress. *New Biol.*, **3**, 825–833.
25. Bauskin,A.R., Alkalay,I. and Ben-Neriah,Y. (1991) Redox regulation of a protein tyrosine kinase in the endoplasmic reticulum. *Cell*, **66**, 685–696.
26. Kanner,S.B., Kavanagh,T.J., Grossmann,A., Hu,S.L., Bolen,J.B., Rabinovitch,P.S. and Ledbetter,J.A. (1992) Sulfhydryl oxidation down-regulates T-cell signaling and inhibits tyrosine phosphorylation of phospholipase Cg1. *Proc. Natl Acad. Sci. USA*, **89**, 300–304.
27. Chae,H.P., Jarvis,L.J. and Uckun,F.M (1993) Role of tyrosine phosphorylation in radiation-induced activation of c-*jun* protooncogene in human lymphohematopoietic precursor cells. *Cancer Res.*, **53**, 447–451.
28. Saito,H. and Streuli,M. (1991) Molecular characterization of protein tyrosine phosphatases. *Cell Growth Diff.*, **2**, 59–65.
29. Liang,C.M., Lee,N., Cattell,D. and Liang,S.M. (1989) Glutathione regulates interleukin-2 activity on cytotoxic T-cells. *J. Biol. Chem.*, **264**, 13519–13523.
30. Bergelson,S., Pinkus,R. and Daniel,V. (1994) Intracellular glutathione levels regulate Fos/Jun induction and activation of glutathione S-transferase gene expression. *Cancer Res.*, **54**, 36–40.
31. Clancy,R.M., Levartrovsky,D., Leszczynsha-Piziak,J., Yegudin,J. and Abramson,S.B. (1994) Nitric oxide reacts with intracellular glutathione and activates the hexose monophosphate shunt in human neutrophils: evidence for S-nitrosoglutathione as a bioactive intermediary. *Proc. Natl Acad. Sci. USA*, **91**, 3680–3684.
32. Kermack,W.O. and Matheson,N.A. (1957) The effects of some analogues of glutathione on the glyoxalase system. *Biochem. J.*, **65**, 45–58.

Received on September 12, 1995; revised on December 15, 1995; accepted on December 21, 1995